EPA-650/4-75-017

May 1975

Environmental Monitoring Series

EFFECTS OF ATMOSPHERIC AEROSOLS ON INFRARED IRRADIANCE AT THE EARTH'S SURFACE IN A NONURBAN ENVIRONMENT

U.S. Environmental Protection Agency
Office of Research and Development
National Environmental Research Center
Research Triangle Park, N. C. 27711

ERRATA

Page 6, line 7 should read "is the Stefan-Boltzman constant and T is the absolute temperature measured"

Page 15 (Figure 3-1) and page 22 (Figure 3-2) "(μ)" should be deleted from the abscissa labels

Page 26, line 2 of Table 3-2 legend should read "READINGS (1/km) AND TURBIDITY (1/optical air mass)"

EPA-650/4-75-017

EFFECTS OF ATMOSPHERIC AEROSOLS ON INFRARED IRRADIANCE AT THE EARTH'S SURFACE IN A NONURBAN ENVIRONMENT

by

Michael R. Riches

Department of Geosciences
North Carolina State University
Raleigh, North Carolina

James T. Peterson and Edwin C. Flowers

Meteorology Laboratory

Program Element No. 1AA009
ROAP No. 26AAS

Prepared for

ENVIRONMENTAL PROTECTION AGENCY
Office of Research and Development
National Environmental Research Center
Research Triangle Park, N. C. 27711

May 1975

James T. Peterson and Edwin C. Flowers are on assignment from the National Oceanic and Atmospheric Administration, U.S. Department of Commerce.

RESEARCH REPORTING SERIES

Research reports of the Office of Research and Development, U.S. Environmental Protection Agency, have been grouped into series. These broad categories were established to facilitate further development and application of environmental technology. Elimination of traditional grouping was consciously planned to foster technology transfer and maximum interface in related fields. These series are:

1. ENVIRONMENTAL HEALTH EFFECTS RESEARCH
2. ENVIRONMENTAL PROTECTION TECHNOLOGY
3. ECOLOGICAL RESEARCH
4. ENVIRONMENTAL MONITORING
5. SOCIOECONOMIC ENVIRONMENTAL STUDIES
6. SCIENTIFIC AND TECHNICAL ASSESSMENT REPORTS
9. MISCELLANEOUS

This report has been assigned to the ENVIRONMENTAL MONITORING series. This series describes research conducted to develop new or improved methods and instrumentation for the identification and quantification of environmental pollutants at the lowest conceivably significant concentrations. It also includes studies to determine the ambient concentrations of pollutants in the environment and/or the variance of pollutants as a function of time or meteorological factors.

This document is available to the public for sale through the National Technical Information Service, Springfield, Virginia 22161.

Publication No. EPA-650/4-75-017

CONTENTS

LIST OF FIGURES

LIST OF TABLES

ABSTRACT

Atmospheric aerosols can affect the surface radiative energy budget through their effects on solar (0.3 to 3.0 micrometers) and infrared (3 to 50 micrometers) radiative transfer. While many studies have focused on the relation between aerosols and observed solar radiation, very few in situ measurements have been simultaneously made of aerosol amounts and infrared radiation. This report describes a study designed to measure hemispheric infrared downward-directed irradiance at the earth's surface and ambient aerosol concentrations at Research Triangle Park, North Carolina. A Funk type net radiometer (with a blackened cavity on the underside) was used to measure the incident all-wave energy. From the value obtained, the observed solar radiation was subtracted to determine the infrared component. The expected incident infrared irradiance was calculated from prevailing atmospheric conditions. Six methods were used for these calculations: four empirical equations based on surface conditions, the Yamamoto chart, and a radiative transfer program using vertical profiles of temperature and moisture.

The observed-minus-calculated downwelling irradiances were then compared to concurrent measurements of the turbidity obtained with a Volz sunphotometer, nephelometer-indicated atmospheric extinction coefficient, and relative humidity. These measurements were analyzed by least-squares regression to determine the extent to which incident hemispheric infrared radiation is affected by varying amounts of

atmospheric aerosols and relative humidity. The results suggested that for a typical hazy summer afternoon with 0.250 turbidity and 0.2 km^{-1} extinction coefficient the excess downward-directed irradiance was approximately 0.03 langley per minute, which is some 6 percent of typical downward infrared irradiances. A nonlinear dependence of excess downwelling irradiance on relative humidity was also suggested.

EFFECTS OF ATMOSPHERIC AEROSOLS ON INFRARED IRRADIANCE AT THE EARTH'S SURFACE IN A NONURBAN ENVIRONMENT

SECTION 1. INTRODUCTION AND LITERATURE REVIEW

INTRODUCTION

Atmospheric aerosols can influence the surface radiative energy budget through their effects on solar (0.3 to 3.0 micrometers (μm) wavelength) and terrestrial infrared (3 to 50 μm wavelength) radiative transfer. Many studies have focused on the relation between aerosol concentrations and observed solar radiation; for example, Robinson (1962), Flowers and Viebrock (1965), McCormick and Ludwig (1967), Paltridge and Platt (1972), and Idso (1972b). Investigators have, however, made very few in situ measurements simultaneously of aerosol concentrations and infrared radiation. The study covered in this report was designed to provide insight into the relation between ambient aerosol concentrations and hemispheric infrared irradiance incident at the earth's surface.

Measurements of hemispheric infrared downward-directed radiation (HIDR) at the earth's surface, along with turbidity and nephelometer readings (indicators of atmospheric aerosol concentrations), were taken during cloud-free conditions. The expected HIDR for an aerosol-free

atmosphere was also calculated at each observation time. On the basis of a comparison of the observed-minus-calculated irradiances with the turbidity and nephelometer readings, the interdependence of these quantities was studied.

LITERATURE REVIEW

One of the first references to the effect of aerosols on the infrared irradiance may be found in the literature of more than 20 years ago, as Robinson (1950) noted a variable component of up to 10 percent in his measurements of HIDR. He ascribed this variation to atmospheric aerosols. Increased aerosol concentrations were associated with increased HIDR. Sheppard (1958) calculated the expected HIDR for an aerosol-free atmosphere and compared these calculated values to measured infrared irradiances. His calculations showed about a 10 percent excess in the HIDR as compared to an aerosol-free atmosphere, which agreed with Robinson's conclusions.

More recently, measurements and theoretical studies of the influence of atmospheric dust on infrared radiation over Northwest India (Peterson and Bryson, 1968; Sargent and Beckman, 1973; and Lal, 1973) have shown an increase in infrared irradiance at the earth's surface apparently due to the dust. Using dust profiles and meteorological data obtained over the Rajasthan Desert, Sargent and Beckman found as much as a 20 percent increase in HIDR as compared to that calculated for a dust-free atmosphere. They also found that the increase shown by the model was highly dependent on the amounts and vertical distribution of the aerosol. The basic results of all three studies indicated that the three primary effects of the aerosol

were a decrease in the upward infrared flux, an increase in downward infrared flux, and a decrease in the net infrared flux, compared to a dust-free atmosphere.

Other studies on wind-blown dust (Idso, 1972a; 1973) at Phoenix, Arizona, also have shown a significant increase in HIDR apparently due to the dust. Idso found a 12 percent increase for a winter dust storm and a 4.3 percent increase for a summer dust storm, reemphasizing Robinson's earlier conclusions. Staley and Jurica (1972) computed the effective atmospheric emissivity for an aerosol-free atmosphere. Measurements made in conjunction with their study suggested additional HIDR from aerosols. From aircraft spectral measurements at 8.5 μm to 16 μm over desert terrain, Hovis et al. (1968) also determined that aerosols have a significant effect on the emissivity of the atmosphere.

Not all researchers agree that increased concentrations of atmospheric aerosols result in significantly increased HIDR. Primarily, the lack of data on aerosol absorption and scattering coefficients in the infrared region have handicapped modelers and forced assumptions that may not be totally realistic. Rasool and Schneider (1971) included aerosols in their climatic model, but found little effect on the infrared flux. Other climatic modelers (e.g., Mitchell, 1971) have chosen to assume that aerosols have little or no effect on infrared radiative transfer. In a dense haze (continental origin) over the sea at Coff's Harbour, Australia, Paltridge and Platt (1972) found no increase in the HIDR as compared to clear-sky data taken on an earlier expedition (Platt, 1972). Their computations also verified this result.

Recently, two studies of urban-rural variations in HIDR have been reported in the literature. Oke and Fuggle (1972) measured this parameter at night, but ascribed the excess HIDR in the urban environment to warmer atmospheric temperatures, instead of to aerosols. At Hamilton, Ontario, Canada, Rouse et al. (1973) measured the HIDR at a rural and an urban site over a 3-year period. Their data indicated a significant increase in the HIDR during the day at the urban site as compared to the rural site. Little difference was found at night. The incident all-wave (solar plus infrared) radiation was about the same for both stations. The authors ascribed these observations to higher relative emissivities because of heavy particulate loading in the urban atmosphere.

The absorption and emission of infrared radiation by different substances are wavelength dependent. This wavelength dependence results in the so-called atmospheric window (8 μm to 12 μm). In this region the two major absorbers of infrared radiation, water vapor and carbon dioxide, do not influence infrared radiation. Thus, it is in the atmospheric window that aerosols can most readily affect infrared radiative transfer. On the basis of their spectral absorption characteristics, there is reason to expect that aerosols will influence infrared transfer. For example, clay minerals (Flanigan and Delong, 1970) and silica (Peterson and Weinman, 1969) are natural substances that have absorption bands in the atmospheric window. Man-made substances such as ammonium sulfate (Neumann, 1972) and carbonaceous materials (Twitty and Weinman, 1971) also have absorption bands in the window region. For aerosols collected mainly from precipitation samples, containing natural and man-made substances, Volz (1972a; 1972b) found the maximum absorption to be in the infrared at 9 μm.

SECTION 2. EXPERIMENTAL DESIGN

INTRODUCTION

The basic experiment consisted of coincident measurements, during cloud-free conditions, of hemispheric infrared (3 to 50 μm) downward-directed radiation (HIDR) at the earth's surface, and of measurements of indicated atmospheric aerosol concentrations from turbidity and nephelometer readings. At each observation time, the expected HIDR for an aerosol-free atmosphere was also calculated from surface temperature and dew point or radiosonde data as appropriate for the calculation scheme. The observed turbidity and nephelometer readings were then compared to the observed-minus-calculated irradiances, and thus the interdependence of these quantities was studied.

RADIATION INSTRUMENTS

To determine the HIDR at the earth's surface, two types of instruments were used. The net all-wavelength radiation was measured by the Funk (CSIRO) type net all-wavelength radiometer (Funk, 1959), with the polyethylene dome from the bottom side replaced by a blackened cavity. The inside temperature of the cavity was continuously monitored with a thermocouple so that the instrument effectively measured the unidirectional irradiance. Three such instruments were used during the course of study. The downward-directed solar irradiance was measured independently by an Eppley Precision Spectral Pyranometer with a WG7 clear-glass dome, transparent from a wavelength of about 0.3 μm to 3.0 μm. The downward-directed infrared

component was then determined from the following relation:

$$NET = SW\downarrow - SW\uparrow + LW\downarrow - TC \qquad (2.1)$$

where NET is the reading from the Funk instrument, SW↓ is the downward-directed solar irradiance from the Eppley instrument, and LW↓ is the HIDR to be determined. TC is the upward-directed infrared irradiance measured by the thermocouple in the blackened cavity (i.e., σT^4, where σ is the Stefan-Boltzman constant and absolute T is the temperature measured by the thermocouple), and SW↑ is the upward-directed solar radiation, which is zero (cavity covering lower sensor). Thus, the HIDR was calculated as follows:

$$LW\downarrow = NET - SW\downarrow + TC \qquad (2.2)$$

CALIBRATION OF RADIATION SENSORS

To field check the calibration of the Eppley Pyranometer, the direct component of the solar beam was shaded with a disc designed to shade out a solid angle of 5° 43'. The change in output of the pyranometer (millivolts) was then divided by the output of the Eppley Normal Incidence Pyrheliometer ($Cal/cm^2\text{-}min^{-1}$) with a similar aperture.

The sun shade method was also used to calibrate the CSIRO radiometers (Funk, 1961; and Latimer, 1963). The error associated with the calibration constant thus determined was on the order of ±5 percent. This value was estimated to include ±1.5 percent error for non-cosine instrument response*

*An instrument is said to have perfect cosine response if the energy from the direct solar beam falling on the horizontal sensing surface of area A is equal to the energy in the area normal to the direct solar beam multiplied by cos Ø. The angle Ø is the solar zenith angle. If the instrument cosine response is perfect, this relation will hold for all Ø and for all possible solar paths across the sensing surface of the instrument.

(Funk, 1959), ±1 percent error for reading stripcharts, and a cumulative ±2.5 percent error for the shade technique (such as instrument overshoot and lag errors (Latimer, 1963), errors in the Pyrheliometer and errors in the mechanics of shading the instrument). A complete discussion of calibration techniques and results was presented by Riches (1974).

MEASUREMENT OF AEROSOLS

The atmospheric aerosol content was estimated in two ways: by measurements with a sunphotometer (Flowers et al., 1969) and an integrating nephelometer (Charlson et al., 1969). Both devices are based on light-scattering principles, and have an effective wavelength of approximately 0.5 μm for the sunphotometer and the nephelometer. If the ambient aerosol followed a Junge (1955) size distribution, few particles outside the range 0.1 to 1.0 μm in radius would affect the sunphotometer or nephelometer measurements. Even though the most efficient particles for infrared emission would likely be somewhat larger than this effective size range because of the longer wavelengths of the emitted energy, these aerosol monitoring techniques were selected because of their ease of operation and instantaneous output.

The sunphotometer measures the solar intensity at 0.5 μm to yield the atmospheric turbidity, or aerosol extinction coefficient, through the relation

$$I_\lambda = I_{o\lambda} \cdot 10^{-(\tau_{r\lambda} + \tau_{3\lambda} + B_\lambda)\, m} \qquad (2.3)$$

where I_λ is the irradiance at wavelength, λ, at the observing point; $I_{o\lambda}$ is the extraterrestrial irradiance at wavelength, λ; $\tau_{r\lambda}$ is the (known) scattering coefficient for air molecules; $\tau_{3\lambda}$ is the (known) absorption coefficient for ozone; B_λ is the turbidity coefficient (to be determined);

and m is the optical air mass (path length of the direct solar beam in the atmosphere) adjusted for atmospheric pressure at the observer's location. The atmospheric turbidity thus obtained is representative of the entire vertical extent of the atmosphere above the observer.

The nephelometer measures the aerosol extinction coefficient by continuously drawing ambient air into a chamber where the extinction coefficient is determined by light scatter. Thus, this measurement is representative of very local conditions. Actually, the extinction coefficient is dependent on scattering and absorption by both gases and aerosols. At 0.55 μm (the effective wavelength of the nephelometer), however, aerosol scattering is almost always the dominant factor affecting the extinction coefficient.

CALCULATION OF THE DOWNWARD-DIRECTED INFRARED IRRADIANCE

There are basically three ways to calculate the expected HIDR. The first method is to use an empirical equation obtained from a regression analysis of actual incoming infrared flux measurements. Usually temperature and water vapor pressure (e.g., Brunt, 1932) or temperature alone (e.g., Swinbank, 1963) are used as independent variables in the regression analysis. Temperature is suggested as a variable by the Stefan-Boltzmann law, which states that a perfect absorber-emitter should emit a radiant flux proportional to the fourth power of its temperature. The exact relation

$$B = E\sigma T^4 \qquad (2.4)$$

where: B is the radiant flux, E is the emissivity, σ is the Stefan-Boltzmann constant, and T is the temperature of the emitter; for $\sigma = 0.817 \times 10^{-10}$ ly/(min - $^{\circ}K^4$), where T is in degrees Kelvin. Water vapor pressure

is also important since water vapor is the major absorber and emitter of atmospheric infrared radiation.

The second and third methods involve the solution of the equations of radiative transfer either by a chart (e.g., Elsasser, 1942; Yamamoto, 1952) or by computer (e.g., Atwater, 1966). The derivation of the equations of radiative transfer is available from several sources (e.g., Kondratyev, 1969). These methods usually treat absorption by water vapor, carbon dioxide, and possibly ozone. The vertical distribution of temperature and water vapor is obtained from radiosonde data, and carbon dioxide is usually considered well-mixed throughout the entire atmospheric column. The resultant infrared irradiances are for an aerosol-free atmosphere.

For this study, six schemes were used to calculate the expected HIDR, since there is no standard method. Four of the methods were semi-empirical equations of Swinbank (1963), Idso and Jackson (1969), Brunt (1932), and Geiger (1965). The equations of Swinbank and of Idso and Jackson are based on surface temperature only, while those of Brunt and Geiger have both surface temperature and water vapor pressure as the independent variables. The original derivations of these four equations were based on best-fit regression curves to actual infrared measurements and thus were representative of an atmosphere containing some aerosols. The equations used with the appropriate constants (Morgan et al., 1971) are given below:

Geiger: $R = E\sigma T^4 [a - b \cdot \exp(-2.3\ ce_2)]$ (2.5)

$a = 0.82\ b = 0.25\ c = 0.094$

Brunt: $R = E\sigma T^4 (a + b\sqrt{e_2})$ (2.6)

$a = 0.605$ $b = 0.048$

Swinbank: $R = E\sigma\, a\, T^6$ (2.7)

$a = 9.35 \times 10^{-6}$

Idso and Jackson: $R = E\sigma T^4 [1 - c \cdot \exp(-d\,(273.16-T)^2)]$ (2.8)

$c = 0.261$ $d = 0.000777$

Where:

E = longwave emissivity assumed to be 1.0

σ = Stefan-Boltzmann Constant = 0.817×10^{-10} ly/(min-$^\circ K^4$)

T = air temperature ($^\circ$K) at 2 m

e_2 = water vapor pressure (mb) at 2 m

The fifth and sixth techniques were based on the equations of radiative transfer. In one method, the investigators used the algorithms of Sasamori (1968), which are based on the Yamamoto chart (Yamamoto, 1952). The algorithms included transmission functions for water vapor, carbon dioxide, and ozone. With the inclusion of ozone, it was believed that the Yamamoto chart was the most theoretically correct of the chart solutions available. This belief was the basis for its selection as one of the six schemes for calculating the expected HIDR. The final method involved a computer solution of the radiative transfer equation (Atwater, 1966), based on the water vapor and carbon dioxide transmission functions of Davis and Viezee (1964). Standard atmospheric distributions of ozone and carbon dioxide were used as input for these last two computational schemes.

DATA COLLECTION AND SITE LOCATION

The infrared irradiance measurements were made continuously from April 1972 through August 1973. Data were reduced for this study, however, only when the sky was cloud-free or when thin cirrus did not extend beyond 15 degrees above the horizon. Moreover, the data were evaluated only when turbidity observations were available, which was usually once an hour, 5 days a week. The nephelometer ran continuously from April through July 1972 and from October 1972 through August 1973. The nephelometer data were evaluated only when both turbidity and infrared irradiance measurements were available. At the observation times, surface temperature, dew point, and pressure were taken locally or, when local equipment failed, were estimated from the National Weather Service hourly observations at Raleigh-Durham airport about 5 miles to the east over mostly rural countryside. The upper air profiles of pressure, temperature, and dew point (for input to the fifth and sixth computation schemes) at Research Triangle Park, North Carolina, were estimated for each observation time from the 1200Z and 0000Z radiosondes taken at Greensboro, North Carolina, which is about 60 miles to the west-northwest and is the nearest radiosonde station to Research Triangle Park. Since the radiation measurements were reduced on "clear" days only, at each measurement time the 1200Z radiosonde data were modified in the lower layers by assuming an adiabatic lapse rate and a constant water vapor mixing ratio through the mixing layer. The absolute values of these profiles were determined from observed local surface pressure, temperature, and dew point observations. Unless otherwise indicated by the synoptic situation, a linear time

interpolation for temperature and dew point was used between the 1200Z and 0000Z data above the mixing height.

The platform from which the radiation measurements were made is approximately 23 feet above a mowed grass surface in a nonurban environment. There are few obstructions (trees only) above 5 degrees from the horizon, and there are no obstructions above 10 degrees from the horizon. The temperature, dew point, pressure, nephelometer, and turbidity observations were made 200 feet west of the platform from which the radiation measurements were taken.

SECTION 3. RESULTS

OBSERVED-MINUS-CALCULATED IRRADIANCE AS A FUNCTION OF NEPHELOMETER READINGS AND TURBIDITY

The observed-minus-calculated irradiance was analyzed as a function of both the sunphotometer- and nephelometer-indicated atmospheric aerosol content for all data collected from April 1972 through August 1973. There were 296 data points for the turbidity comparisons and 231 data points for the nephelometer comparisons. The data were stratified three ways for each type of aerosol measurement. First, all data were considered. Then the data were printed out chronologically by the computer, along with the reported sky condition at the time of observation. The May-through-September period for both 1972 and 1973 contained the majority of reported hazy sky conditions. On this basis, May through September was designated the "hazy" season (177 data points) and October through April was designated the "clean" season (119 data points). For each of the three stratifications and the six calculation schemes, the observed-minus-calculated irradiance was compared to the surface relative humidity, turbidity, and nephelometer readings.

Before the results were analyzed in detail, a cursory study was made of the interrelationship between the values of the infrared irradiance determined by the six empirical or theoretical schemes and the observed data. Infrared irradiance determined by the two formulae based only on surface temperature data (Swinbank and Idso) showed large diurnal variation and highest values during midday. This problem of excessive daytime

estimates has been discussed previously by Paltridge (1970). In general, the computations from the two equations based on surface temperature and vapor pressure and the two techniques using upper-air data were consistent.

All Data

Considering all data, investigators found that positive correlations resulted between nephelometer readings and all six schemes of observed-minus-calculated irradiances. This fact is exemplified by the scatter diagram shown in Figure 3.1, which is a plot of the observed-minus-calculated irradiance versus nephelometer readings. The calculated values were obtained from the Yamamoto chart.

Two points should be made about the data presented in Figure 3.1. First, 80 percent of the measured extinction coefficients are less than 0.2 per kilometer.* This bias results largely from the nonurban environment of the study site. Second, the data show considerable scatter about the regression line. This scatter indicates that the nephelometer readings are not necessarily a reliable measure of the extinction coefficient for infrared radiation. Since nephelometer readings are a measure of the light scatter or extinction coefficient in the visible range, it is possible for the particle size distribution to include excess large (small) particles that significantly affect the infrared (visible) but not the visible (infrared) radiation.

*With the use of the nephelometer factory calibrations, an extinction coefficient of 0.2 km^{-1} is equivalent to a visibility of 23 km and a mass loading of 87 $\mu g\ m^{-3}$.

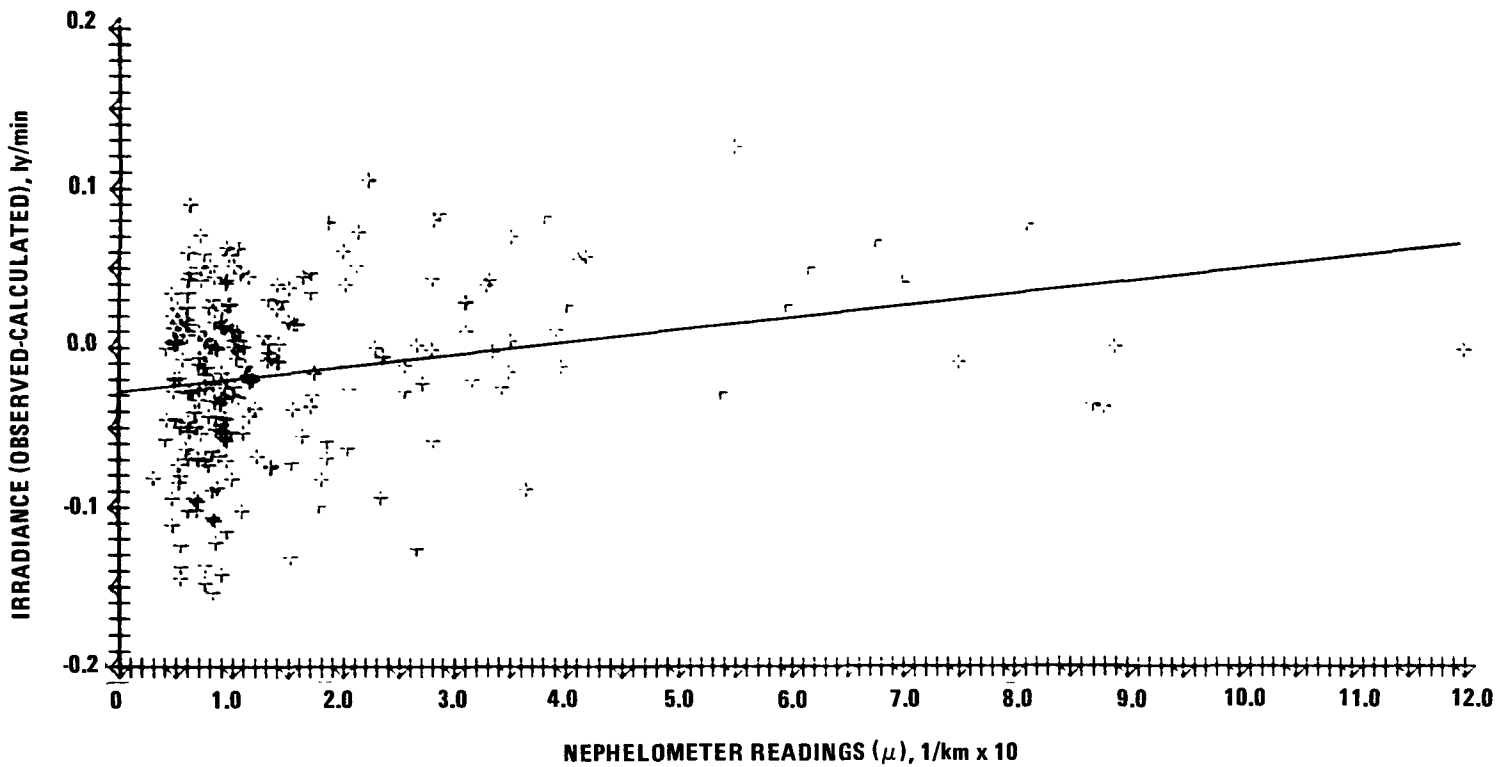

Figure 3-1. Scatter diagram for observed-minus-calculated irradiance versus nephelometer readings (extinction coefficient) for all data (calculated irradiance from the Yamamoto chart).

Other contributions to the scatter shown in Figure 3.1 (and all other diagrams presented herein) are made from several sources. The accuracy of the instruments and the errors introduced during the reduction of the data from these instruments contribute through Equation 2.1. The calculated HIDRs are in error to the extent that the meteorological input data are in error. The formulae themselves are also a source of scatter since they are not perfect predictors of the irradiance, as indicated by the fact there is no standard method for calculating the expected downward irradiance. Lastly, the aerosol measurement techniques contain instrument and data reduction errors that can also contribute to the scatter.

A third point of interest in Figure 3.1 is the negative intercept of the regression line. In Table 3.1 the regression analysis shows that all but the Atwater program have negative intercepts for the linear regression. The negative intercepts are the largest for the two equations having temperature as the sole independent variable (Swinbank and Idso formulae). Next largest are for Brunt and Geiger formulae, which have temperature and water vapor for independent variables. The intercepts for the theoretical schemes are the smallest, with the regression for the Yamamoto chart being negative and the Atwater scheme being positive. Two possible explanations for the negative intercepts follow. First, for summer afternoons, Paltridge (1970) proposed a negative correction of 0.043 ly/min for the Swinbank formula, based on comparisons between that formula and observed data. Paltridge's hypothesis was that the correction is needed because the original formula was obtained from measurements made at night. During daytime, with low-level temperature lapse conditions, the surface temperature is an overestimate of the

Table 3-1. REGRESSION ANALYSIS AND ANALYSIS OF VARIANCE FOR OBSERVED-MINUS-CALCULATED IRRADIANCES (ly/min) VERSUS NEPHELOMETER READINGS (1/km x 10) AND TURBIDITY (1/optical air mass) FOR ALL DATA AND FOR CLEAN AND HAZY SEASONS

Scheme	Slope	Intercept	Std error of slope	Correlation coefficient	Std error of estimate	F test
Irradiance vs. nephelometer for all data						
Idso	0.0179	-0.0676	0.0381	0.27	0.0646	18.4[a]
Swinbank	0.0105	-0.0614	0.0385	0.26	0.0653	17.0[a]
Brunt	0.0058	-0.0384	0.0331	0.17	0.0561	6.9[b]
Geiger	0.0089	-0.0528	0.0340	0.25	0.0577	15.7[a]
Yamamoto	0.0079	-0.0283	0.0309	0.25	0.0523	14.8[a]
Atwater	0.0048	0.0030	0.0272	0.17	0.0462	7.1[b]
Irradiance vs. turbidity for all data						
Idso	0.0566	-0.0583	0.5722	0.10	0.0745	2.9[c]
Swinbank	0.0508	-0.0516	0.5768	0.09	0.0751	2.3
Brunt	0.0057	-0.0311	0.4982	0.01	0.0648	<1
Geiger	0.0552	-0.0466	0.5147	0.11	0.0670	3.4[c]
Yamamoto	0.0498	-0.0230	0.4705	0.11	0.0612	3.3[c]
Atwater	0.0212	0.0067	0.4169	0.05	0.0543	<1
Irradiance vs. nephelometer for clean season						
Idso	0.0296	-0.0664	0.1890	0.15	0.0548	2.6
Swinbank	0.0353	-0.0639	0.1943	0.18	0.0563	3.5[c]
Brunt	0.0122	-0.0255	0.1631	0.07	0.0473	<1
Geiger	0.0145	-0.0403	0.1735	0.08	0.0503	<1
Yamamoto	0.0135	-0.0196	0.1536	0.09	0.0445	<1
Atwater	-0.0010	0.0178	0.1440	0.01	0.0417	<1
Irradiance vs. turbidity for clean season						
Idso	-0.2664	-0.0190	1.5440	0.17	0.0559	3.5[c]
Swinbank	-0.3181	-0.0077	1.6020	0.19	0.0580	4.6[b]
Brunt	-0.3270	0.0150	1.2947	0.24	0.0469	7.5[b]
Geiger	-0.3762	0.0013	1.3779	0.26	0.0499	8.7[a]
Yamamoto	-0.3165	0.0162	1.2073	0.25	0.0437	8.0[b]
Atwater	-0.3329	0.0422	1.0893	0.29	0.0395	10.9[a]

Table 3-1.(continued). REGRESSION ANALYSIS AND ANALYSIS OF VARIANCE FOR OBSERVED-MINUS-CALCULATED IRRADIANCES (ly/min) VERSUS NEPHELOMETER READINGS (1/km x 10) AND TURBIDITY (1/optical air mass) FOR ALL DATA AND FOR CLEAN AND HAZY SEASONS

Scheme	Slope	Intercept	Std error of slope	Correlation coefficient	Std error of estimate	F test
Irradiance vs. nephelometer for hazy season						
Idso	0.0154	-0.0926	0.0328	0.42	0.0683	26.9[a]
Swinbank	0.0154	-0.0882	0.0325	0.43	0.0678	27.3[a]
Brunt	0.0110	-0.0660	0.0276	0.37	0.0576	19.2[a]
Geiger	0.0138	-0.0788	0.0266	0.44	0.0590	29.1[a]
Yamamoto	0.0116	-0.0484	0.0266	0.40	0.0554	23.4[a]
Atwater	0.0078	-0.0123	0.0230	0.32	0.0480	14.0[a]
Irradiance vs. turbidity for hazy season						
Idso	0.1464	-0.0879	0.5814	0.24	0.0818	11.1[a]
Swinbank	0.1490	-0.0839	0.5762	0.25	0.0811	11.7[a]
Brunt	0.1038	-0.0636	0.5004	0.20	0.0704	7.5[b]
Geiger	0.1535	-0.0785	0.5128	0.29	0.0721	15.7[a]
Yamamoto	0.1263	-0.0476	0.4823	0.25	0.0679	12.0[a]
Atwater	0.0838	-0.0131	0.4269	0.19	0.0601	6.7[b]

[a]Significant at 99.5 percent confidence level.
[b]Significant at 95 percent confidence level.
[c]Significant at 90 percent confidence level.

effective radiating temperature of the atmosphere. He also suggests applying the correction to other formulae calibrated with night measurements of infrared radiation. Although this correction can vary with time of day and with season, the magnitude of the proposed correction is large enough to decrease significantly or change the sign on the intercepts presented.

The second possible explanation stems from the empirical nature of the first four computational schemes. Since they were derived from HIDR observations, these schemes represent an atmosphere in which the

aerosol content is not zero, but some higher value. Thus, one would not expect the observed-minus-calculated differences to be zero at zero aerosol concentration, but at some higher value. In other words, a negative intercept for the empirical schemes is realistic if aerosols do, in fact, significantly alter the HIDR.

The slopes, or coefficients of the independent variable, for all six linear regressions presented in Table 3.1 (irradiance vs. nephelometer for all data) are positive and statistically significant at least at the 95 percent confidence level as determined by a standard F-test. Four of the schemes (Idso, Swinbank, Geiger, and Yamamoto) are significant at the 99.5 percent confidence level. This fact suggests an excess of HIDR over that expected for an aerosol-free atmosphere. The correlation coefficients range from 0.17 for the Atwater and Brunt schemes to 0.27 for the Idso scheme. Note also that in each case the standard error of the slope and the standard error of estimate are large. This is a reflection of the scatter of the data, as pointed out earlier in the discussion.

Similar regression statistics for the observed-minus-calculated irradiances as a function of turbidity are presented in Table 3.1 (irradiance vs. turbidity for all data). The positive slopes of the regression lines are significantly different from zero at the 90 percent level for only three of the schemes, which are the formulae of Idso and Geiger and the Yamamoto chart. Moreover, all the schemes have low correlation coefficients and large standard errors of slope. The large scatter results in part from the fact that turbidity, like the nephelometer scattering coefficient, is not necessarily a reliable measure of the extinction coefficient in the infrared and in part from the calculation

and observational errors discussed previously. The negative intercepts (Table 3.1 - irradiance vs. turbidity for all data) again suggest an overestimate for the calculated daytime HIDR.

Another reason for the large data scatter is that turbidity is a measure of the extinction in the entire atmospheric column, whereas the nephelometer readings represent the local ground-level extinction coefficient. Since about 75 percent of the HIDR typically originates in the lowest 400 meters of the atmosphere (Sellers, 1965), nephelometer readings might be expected to be better correlated to the excess irradiance than turbidity is.

Clean Season Data

Data for the clean season (October through April) were generally inconclusive. The regression analyses for the observed-minus-calculated irradiances as a function of extinction coefficient and turbidity are presented in Table 3.1 (irradiance vs. nephelometer for the clean season and irradiance vs. turbidity for the clean season, respectively). The data had a strong bias toward low values of turbidity and extinction coefficient and large scatter about the regression lines. The generally poor results were likely because the data clustered about low aerosol values resulting from the generally clean, dry atmospheric conditions. Moreover, the large scatter also resulted from (1) the use of turbidity and the extinction coefficient in the visible range to represent the infrared extinction coefficient; (2) the fact that turbidity is a weak function of the lower atmospheric layer responsible for the majority of the HIDR, as discussed earlier; and (3) the observational and calculation errors.

Hazy Season Data

The regression analysis and the analysis of variance for the observed-calculated irradiance as a function of nephelometer readings for the hazy season (May through September) are presented in Table 3.1 (irradiance vs. nephelometer for the hazy season). Note that the positive slopes for all six schemes are significantly different from zero at the 99.5 percent confidence level and that the standard error of the slope is smaller than that for the slope in the cases discussed previously. Correlation coefficients are about three times larger than those obtained for the clean season data, and twice that obtained for the total data set. The more significant statistical results from the hazy season suggest that the narrow range of aerosol concentrations during the clean period was not sufficient to elucidate an aerosol-irradiance relation.

The intercept for all six regression equations is negative (see Table 3.1 - irradiance vs. nephelometer for the hazy season). As discussed previously, this fact is not unrealistic for the empirical schemes, but could be because of an overestimate of the infrared irradiance by the schemes for daytime observations. The scatter of the data about the regression as shown in Figure 3.2 is also large for these hazy-season measurements.

In contrast to the statistics presented for the clean season, the statistics for the irradiance differences as a function of turbidity during the hazy months (Table 3.1 - irradiance vs. turbidity for the hazy season) show a positive slope that is significantly different from zero at least at the 95 percent confidence level for all six schemes. The standard error of the slope is the smallest yet found for turbidity regressions. The wider and more evenly distributed range of turbidity

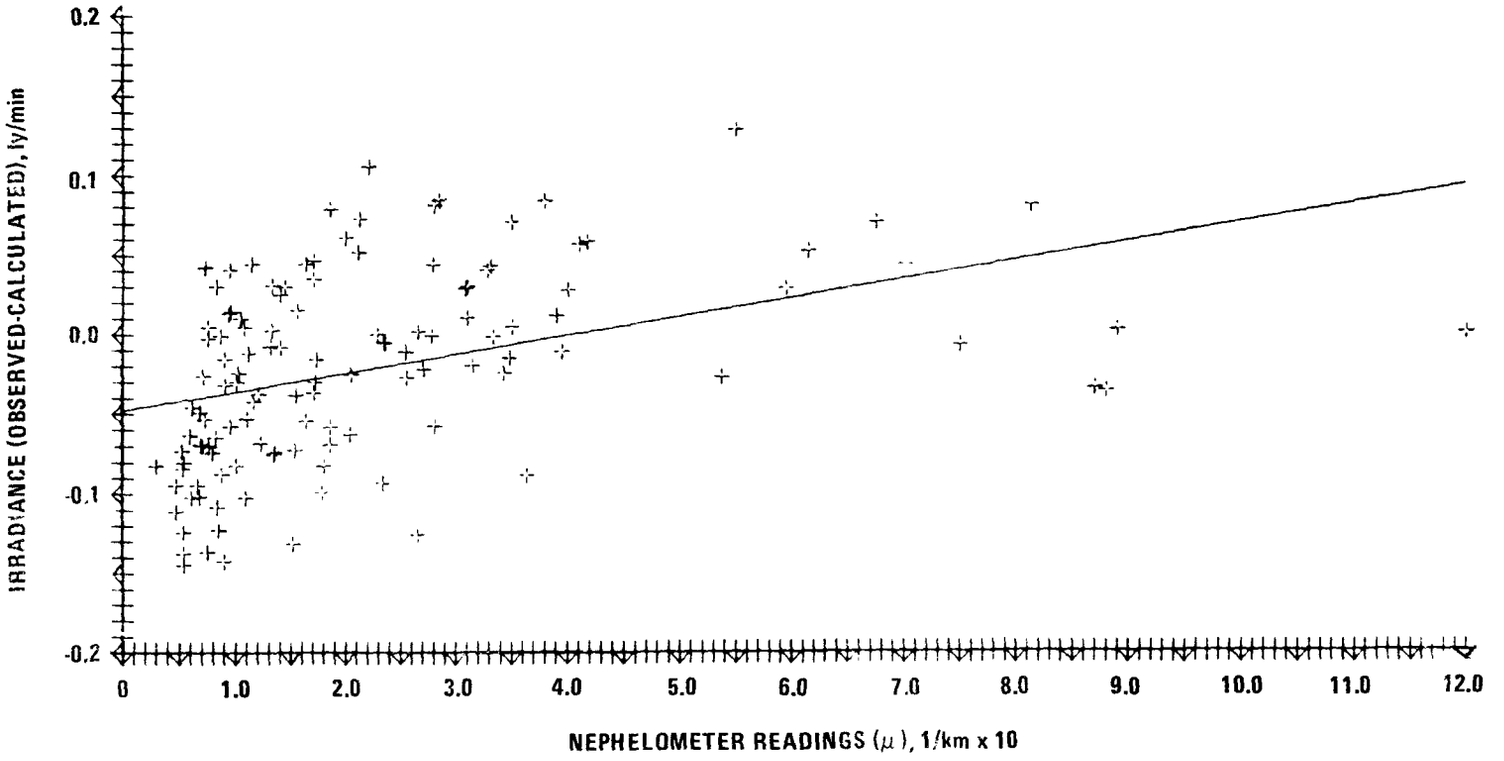

Figure 3-2. Scatter diagram for observed-minus-calculated irradiance versus nephelometer readings (extinction coefficient) for the hazy season (calculated irradiance from the Yamamoto chart).

values (see example scatter diagram in Figure 3.3) allows more physical significance to be given to the positive slopes found for the hazy season, even though considerable scatter about the regression line is still present. Similar to the regression on nephelometer readings for the hazy season, the correlation coefficients are about twice as large as those found for the total data set, averaging about 0.24. They are smaller, however, than those found for the nephelometer readings. These facts show that turbidity is more indicative of the lower-atmospheric aerosol concentration during the hazy season than during the clean season, but that it is not as reliable a measure as the nephelometer readings.

The wider and more evenly distributed range of turbidity values and nephelometer readings found for the hazy-season data allow a discussion of the physical meaning of the regression equations derived earlier. If the six results of the observed-minus-calculated irradiance are used as

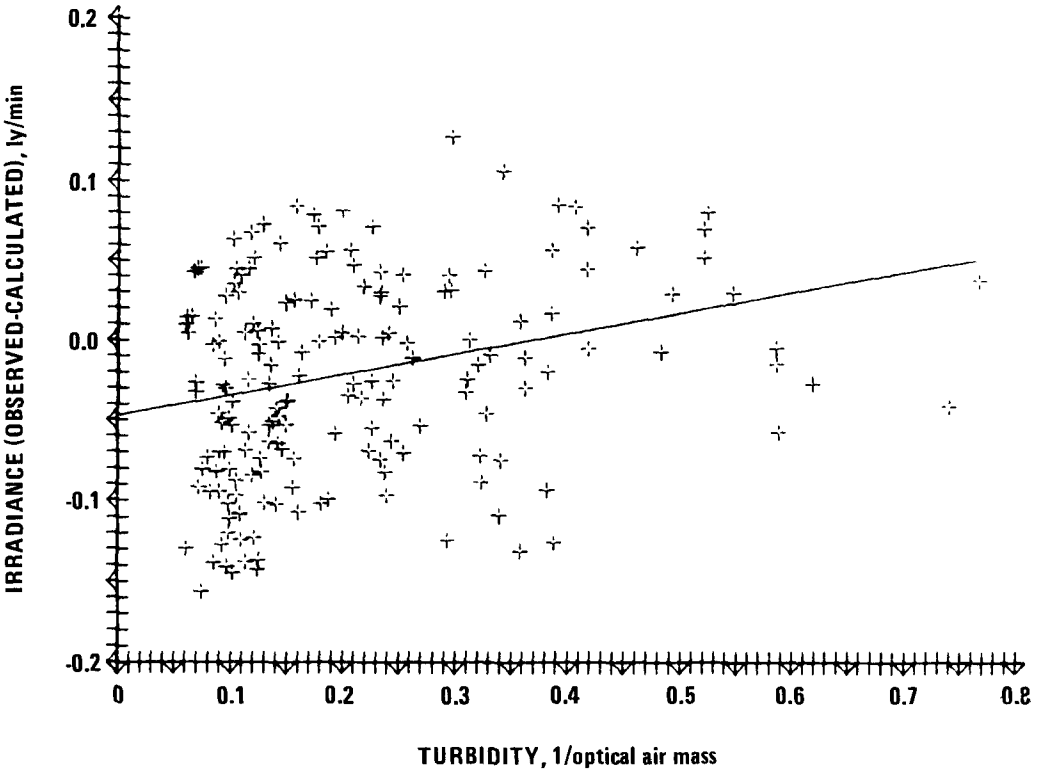

Figure 3-3. Scatter diagram for observed-minus-calculated irradiance versus turbidity for the hazy season (calculated irradiance from the Yamamoto chart).

a function of nephelometer readings (extinction coefficient [km^{-1}]) during the hazy season, the average slope of the regression line is 0.125 (ly/km-min). Thus, the results presented herein indicate that an ambient low-level atmospheric aerosol concentration with extinction coefficient of 0.1 km^{-1} would increase the HIDR by 0.0125 ly/min. For a typical summer afternoon with an extinction coefficient of 0.2 km^{-1}, the excess irradiance is 0.025 ly/min. The average slope from the six schemes for the data of all seasons (with nephelometer readings considered) is 0.093 ly/km-min.

The average slope of the linear regression line between the irradiance difference during the hazy season and the turbidity coefficient is 0.127 ly/optical air mass-min. Thus, for a typical summer afternoon in North Carolina with a turbidity of 0.250, which is similar to a nephelometer extinction coefficient of 0.2 km^{-1}, the excess downward irradiance would be 0.032 ly/min. This value (0.032 ly/min) represents about 6 percent of the typical HIDR total.

RELATIVE HUMIDITY RESULTS

It has been established that relative humidity is an important parameter in aerosol growth. For example, Covert et al. (1972) and Winkler (1973) have shown that ambient aerosols grow as relative humidity increases. Since the absorption coefficient for aerosols depends directly on its radius (Deirmendjian, 1969), the increased particle size should increase the particle absorption (or emission) in the infrared. The adsorbed or absorbed water should also increase the particle absorption (or emission) since water is an effective absorber in the infrared (Kondratyev, 1969). Thus, relative humidity should correlate with the observed-minus-calculated HIDR. Since scatter by aerosols is proportional

to particle size (Kondratyev, 1969), nephelometer readings and turbidity should also correlate with the surface relative humidity. To test these hypotheses, the observed-minus-calculated HIDR, turbidity, and nephelometer data were analyzed by least-square linear regression as a function of surface relative humidity.

In Table 3.2, the regression analyses and analyses of variance are presented for all data, and for clean and hazy stratifications for nephelometer readings and turbidity as a function of relative humidity. The results are as suggested above. The nephelometer readings are positively correlated with relative humidity for all three stratifications, with correlation coefficients of about 0.55; and the positive slopes are statistically significantly different from zero at the 99.5 percent confidence level, with relatively small standard error of the slopes. Note that the slopes for the clean season are about four times larger than those for the hazy season. This fact may be the result of the bias toward low nephelometer readings during the clean months as discussed previously. This large change in slope is most likely not physically significant. The results for the "hazy" data set are similar to those obtained for all the data.

The results for turbidity as a function of relative humidity are similar to those presented for nephelometer readings. The slopes are positive and significantly different from zero, at least at the 95 percent confidence level; but the correlation coefficients are lower, and the standard errors of slope are larger than the corresponding statistics for the nephelometer readings. Again, the slope for the clean season differs from those obtained for the two other stratifications, and this difference is attributed to the bias toward low turbidity during the clean season.

Table 3-2. REGRESSION ANALYSIS AND ANALYSIS OF VARIANCE FOR NEPHELOMETER READINGS (1/km x 10) AND TURBIDITY (1/optical air mass) VERSUS RELATIVE HUMIDITY (percent) FOR THE THREE STRATIFICATIONS

Scheme	Slope	Intercept	Std error of slope	Correlation coefficient	Std error of estimate	F test
Nephelometer						
All data	5.81	44.6	8.78	0.55	14.9	100.3[a]
Clean season	28.90	22.3	43.55	0.55	12.6	46.2[a]
Hazy season	4.54	50.2	7.08	0.54	14.8	50.3[a]
Turbidity						
All data	59.29	47.4	125.5	0.43	16.3	65.6[a]
Clean season	97.45	41.5	458.0	0.21	16.6	5.3[b]
Hazy season	42.73	53.0	111.6	0.36	15.7	25.6[a]

[a]Significant at 99.5 percent confidence level.
[b]Significant at 95 percent confidence level.

The regression analyses and analyses of variance for the observed-minus-calculated HIDR as a function of relative humidity for all six schemes are presented in Table 3.3 for the total data set, clean season, and hazy season, respectively. All 18 slopes are positive and significantly different from zero at the 99.5 percent confidence level. The correlation coefficients are highest for the Idso and Swinbank schemes and lowest for the Atwater scheme, with the other three schemes in the middle. Since Idso and Swinbank methods do not contain water vapor as an independent variable, the higher correlations may reflect a need to include water vapor as a parameter, rather than a better correlation with particle growth. The seasonal (clean versus hazy) difference in correlation coefficients is the result of the dryer air dominating the clean season. In other words, during the clean season, the absolute

humidity is less than that found during the hazy season, which is frequently influenced by a warm, moist air mass of maritime origin. Thus, high relative humidities during the clean season may not be associated with enough water vapor for significant particle growth.

Table 3-3. REGRESSION ANALYSIS AND ANALYSIS OF VARIANCE FOR OBSERVED-MINUS-CALCULATED IRRADIANCES (ly/min) VERSUS RELATIVE HUMIDITY (percent) FOR ALL DATA AND FOR CLEAN AND HAZY SEASONS

Scheme	Slope	Intercept	Std error of slope	Correlation coefficient	Std error of estimate	F test[a]
All data						
Idso	0.0025	-0.1922	0.0033	0.61	0.0594	173.5
Swinbank	0.0025	-0.1863	0.0033	0.60	0.0601	169.1
Brunt	0.0017	-0.1240	0.0032	0.46	0.0575	79.8
Geiger	0.0020	-0.1485	0.0032	0.52	0.0574	111.2
Yamamoto	0.0017	-0.1139	0.0029	0.51	0.0529	104.4
Atwater	0.0012	-0.0599	0.0027	0.41	0.0495	59.9
Clean season						
Idso	0.0019	-0.1319	0.0027	0.57	0.0464	58.1
Swinbank	0.0020	-0.1300	0.0028	0.59	0.0480	61.2
Brunt	0.0012	-0.0720	0.0026	0.43	0.0438	25.8
Geiger	0.0012	-0.0856	0.0028	0.40	0.0474	22.6
Yamamoto	0.0010	-0.0547	0.0025	0.37	0.0420	18.7
Atwater	0.0006	-0.0132	0.0023	0.27	0.0398	8.9
Hazy season						
Idso	0.0039	-0.3014	0.0031	0.79	0.0521	283.5
Swinbank	0.0039	-0.2953	0.0031	0.79	0.0517	284.6
Brunt	0.0029	-0.2240	0.0031	0.69	0.0522	157.4
Geiger	0.0033	-0.2534	0.0030	0.75	0.0501	220.5
Yamamoto	0.0030	-0.2062	0.0029	0.71	0.0490	184.4
Atwater	0.0022	-0.1331	0.0029	0.61	0.0485	104.0

[a]All data in this column significant at 99.5 percent confidence level.

Secondly, notice the large negative intercept for all 18 cases. This can be accounted for in part by the tendency of the calculation schemes to overestimate the irradiance for daytime observations. The negative intercept may also result from the mechanics of particle growth. Covert et al. (1972) show that particle growth for relative humidities below 60 percent is very small. For relative humidities greater than 60 percent, particle growth increases very rapidly with relative humidity. Figure 3.4 shows the positive correlation between observed-minus-calculated irradiance and relative humidity, which presumably results from aerosol growth dependence on relative humidity. Because the aerosol growth is strongly nonlinearly dependent on humidity, however, a nonlinear curve should be used to fit the data of Figure 3.4. These data do suggest such a curve with wide scatter and little apparent slope at relative humidities less than about 60 percent.

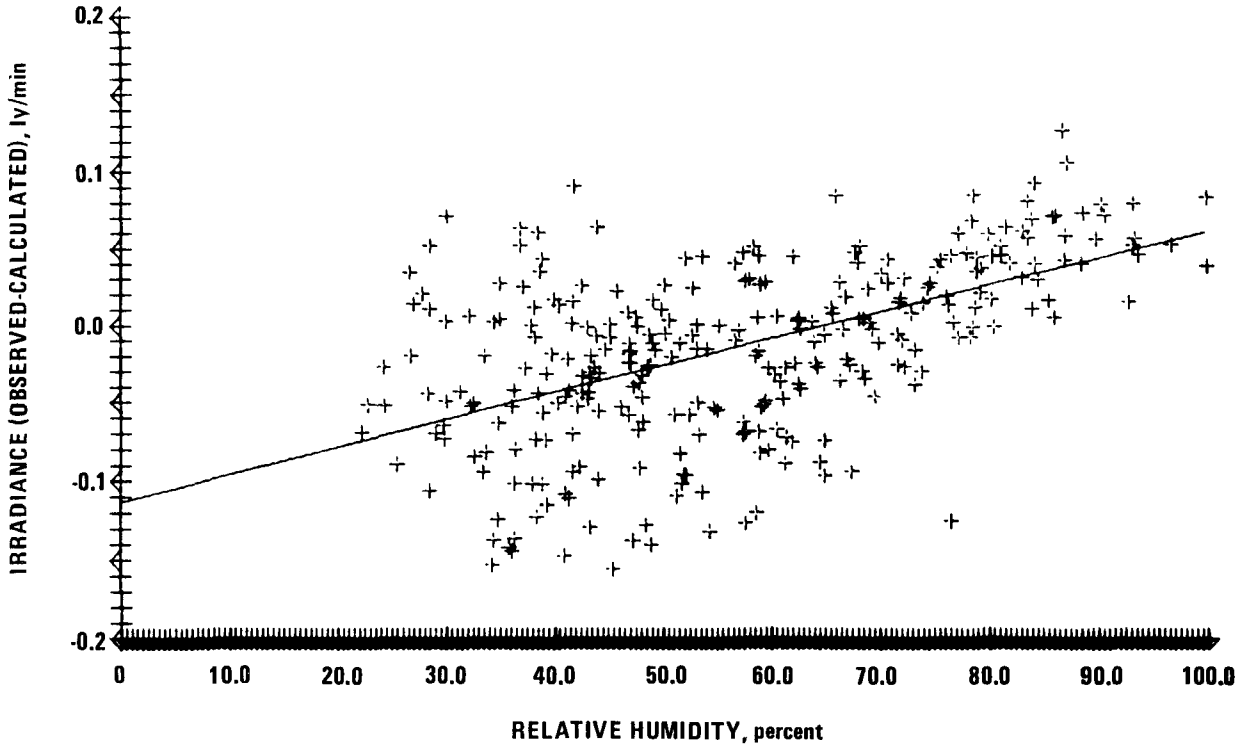

Figure 3-4. Scatter diagram for observed-minus-calculated irradiance versus relative humidity for all data (calculated irradiance from the Yamamoto chart).

SECTION 4. DISCUSSION

Analysis of the data suggests that for a nonurban atmosphere, aerosols can contribute a significant excess of hemispheric infrared downward-directed radiation, particularly in a hazy atmosphere. The results of averaging all six computational schemes together indicated that 0.013 ly/min is produced for each 10th of turbidity, and 0.0125 ly/min is produced for an aerosol concentration equivalent to a nephelometer-indicated extinction coefficient of 0.1 km^{-1}. For a typical summer day with 0.250 turbidity and 0.2 km^{-1} extinction coefficient, the excess irradiance suggested is 0.033 and 0.025, respectively, or approximately 0.03 ly/min on the average. During several summer days in St. Louis, Missouri, Peterson and Flowers (1974) measured urban-rural differences in turbidity of about 0.05, which corresponds to a 0.007 ly/min urban-rural difference in down-welling infrared irradiance. In Los Angeles, however, with considerably higher urban pollution concentrations, they measured turbidity differences through the lowest 1700 meters of the atmosphere of more than 0.2, which corresponds to 0.026 ly/min of excess irradiance.

For the significance of these results to be interpreted in terms of surface energy budgets, they have to be put in proper perspective. During midday in summer, with cloudless conditions in the central U.S., for example, the incident solar irradiance would approximate 1.3 ly/min. Obviously, an excess infrared irradiance of up to 0.03 ly/min would have minor significance during these hours. During nighttime, however, a much different picture emerges. Then, with no solar component, the net radiative

flux at the surface would typically be about -0.1 ly/min (a negative value means a net flux away from the earth). An excess infrared flux resulting from aerosols of 0.03, or even 0.007, ly/min now becomes an important factor.

In terms of a daily radiative energy budget, the following example for the central U. S. in July is illuminating. The average daily receipt of solar radiation is about 600 ly/day. With an albedo of 15 percent, 510 ly/day are absorbed by the ground. A typical net infrared flux of -0.1 ly/min (144 ly/day) would yield a net all-wave radiation receipt of 366 ly/day. The data from this study suggest that an aerosol loading equivalent to a turbidity of 0.2 would cause an additional downward infrared flux of 37 ly/day. A turbidity of 0.05 corresponds to 9 ly/day. Thus, for a clean atmosphere or small urban-rural turbidity difference, on a daily basis, the excess infrared flux would have minor significance. In contrast, higher turbidities, as in the example above, could alter the net radiative flux by some 10 percent.

The data presented herein showed a statistically significant correlation between relative humidity and atmospheric aerosol concentrations as indicated by nephelometer and sunphotometer. This finding presumably reflected the effect of humidity on aerosol growth, especially at higher humidities. The data also showed a significant correlation between observed-calculated HIDR and relative humidity. A nonlinear dependence was suggested by the results. Large scatter and little trend were evident at humidities less than 60 percent; at higher humidities, the excess HIDR increased noticeably as a function of humidity. Thus, relative humidity could also be used as an indicator of excess infrared irradiance.

It is possible, however, that the equations used to calculate the HIDR underestimate the flux at high humidities and the derived relations should be checked further during these conditions.

In summary, the results of this study do indicate that atmospheric aerosols can measurably influence downward-directed infrared radiation. Thus, their infrared radiative effects should be included in certain surface energy budget studies, especially in areas with high aerosol concentrations.

5. LIST OF REFERENCES

Angstrom, A., 1929: On the atmospheric transmission of sun radiation and on dust in the air. Geograph. Ann., Vol. 11, 156-166.

Atwater, M. A., 1966: Comparison of numerical methods for computing radiative temperature changes in the atmospheric boundary layer. J. Appl. Meteor., Vol. 5, No. 6, 824-831.

Brunt, D., 1932: Notes on radiation in the atmosphere. Quart. J. Roy. Meteor. Soc., Vol. 58, No. 247, 389-420.

Charlson, R. J., Ahlquist, N. C., Selvidge, H., and MacCready, P. B., 1969: Monitoring of atmospheric aerosol parameters with the integrating nephelometer. J. APCA., Vol. 19, No. 12, 937-942.

Covert, D. S., Charlson, R. J., and Ahlquist, N. C., 1972: A study of the relationship of chemical composition and humidity to light scattering by aerosols. J. Appl. Meteor., Vol. 11, No. 6, 968-976.

Davis, P. A., and W. Viezee, 1964: A model for computing infrared transmission through atmospheric water vapor and carbon dioxide. J. Geophys. Res., Vol. 69, No. 18, 3785-3794.

Deirmendjian, D., 1969: Electromagnetic Scattering on Spherical Polydispersions. Elsevier Publ. Co., N. Y.

Elsasser, W. M., 1942: Heat Transfer by Infrared Radiation in the Atmosphere. Harvard Meteor. Studies, No. 6, Harvard Univ. Press, Cambridge, Mass.

Flanigan, D. R., and DeLong, H. P., 1970: Spectral absorption characteristics of the major components of dust clouds. Edgewood Arsenal technical report 4430, Dept. of the Army, Edgewood Arsenal, Maryland. (AD 712989).

Flowers, E. C., McCormick, R. A., and Kurfis, K. R., 1969: Atmospheric turbidity over the United States, 1961-1966. J. Appl. Meteor., Vol. 8, No. 6, 955-962.

Flowers, E. C., and Viebrock, H. J., 1965: Solar radiation: an anomalous decrease of direct solar radiation. Science, Vol. 148, No. 3669, 493-494.

Funk, J. P., 1959: Improved polythene-shielded net radiometer. J. Sci. Instruments, Vol. 36, 267-270.

Funk, J. P., 1961: A note on the long-wave calibration of convectively shielded net radiometers. Arch. Meteor. Geoph. Biokl., Ser. B, Vol. 11, No. 1, 70-74.

Geiger, R., 1965: The climate near the ground. Harvard Univ. Press, Cambridge, Mass.

Hovis, W. A., Blaine, L. R., and Callahan, W. R., 1968: Infrared aircraft spectra over desert terrain 8.5 μ to 16 μ. Appl. Optics, Vol. 7, No. 6, 1137-1140.

Idso, S. B., 1972a: Radiation fluxes during a dust storm. Weather, Vol. 27, No. 5, 204-208.

Idso, S. B., 1972b: Solar radiation measurements augment air pollution studies. J. APCA., Vol. 22, No. 5, 364-368.

Idso, S. B., 1973: Thermal radiation from a tropospheric dust suspension. Nature, Vol. 241, No. 5390, 448-449.

Idso, S. B., and Jackson, R. D., 1969: Thermal radiation from the atmosphere. J. Geophys. Res., Vol. 74, No. 23, 5397-5403.

Junge, C., 1955: The size distribution and aging of natural aerosols as determined from electrical or optical data on the atmosphere. J. Meteor., Vol. 12, No. 1, 13-25.

Kondratyev, K. Ya., 1969: Radiation in the Atmosphere. Academic Press, New York.

Lal, M., 1973: Terrestrial radiation balance in the atmosphere over NW-India. Arch. Meteor. Geoph. Biokl., Ser. B, Vol. 21, No. 2-3, 233-242.

Latimer, J. R., 1963: The accuracy of total radiometers. Symposium on the heat exchange at snow and ice surfaces, 26 October 1962. National Research Council of Canada, Associate Committee on Soil and Snow Mechanics, Tech. Memo, No. 78.

McCormick, R. A., and Ludwig, J. H., 1967: Climate modification by atmospheric aerosols. Science, Vol. 156, No. 3780, 1358-1359.

Mitchell, J. M., 1971: The effect of atmospheric aerosols on climate with special reference to temperature near the Earth's surface. J. Appl. Meteor., Vol. 10, No. 4, 703-714.

Morgan, D. L., Pruitt, W. O., and Lourence, F. J., 1971: Estimations of atmospheric radiation. J. Appl. Meteor., Vol. 10, No. 3, 463-468.

Neumann, J., 1972: Radiation absorption by droplets of sulfuric acid water solutions and by ammonium sulfate particles. Department of Atmospheric Sciences. The Hebrew University of Jerusalem, Israel.

Oke, T. R., and Fuggle, R. F., 1972: Comparison of urban/rural counter and net radiation at night. Bound.-Layer Meteor., Vol. 2, No. 3, 290-308.

Paltridge, G. W., 1970: Day-time long-wave radiation from the sky. Quart. J. Roy. Meteor. Soc., Vol. 96, No. 410, 645-653.

Paltridge, G. W., and Platt, C. M. R., 1972: Absorption and scatter of radiation by an aerosol layer in the free atmosphere. J. Atmos. Sci., Vol. 30, No. 4, 734-737.

Peterson, J. T., and Bryson, R. A., 1968: The influence of atmospheric particulates on the infrared radiation balance of Northwest India. Proc. 1st. National Conf. on Weather Modification, Albany, New York.

Peterson, J. T., and Flowers, E. C., 1974: Urban-rural solar radiation and aerosol measurements in St. Louis and Los Angeles. Preprints, A.M.S. Symposium on Atmospheric Diffusion and Air Pollution, Santa Barbara, Calif., 129-132.

Peterson, J. T., and Weinman, J. A., 1969: Optical properties of quartz dust particles at infrared wavelengths. J. Geophys. Res., Vol. 74, No. 28, 6947-6950.

Platt, C. M. R., 1972: Airborne infrared radiance measurements (10 to 12 micron wavelength) off tropical East-Coast Australia. J. Geophys. Res., Vol. 77, No. 9, 1597-1609.

Rasool, S. I., and Schneider, S. H., 1971: Atmospheric carbon dioxide and aerosols: effects of large increases on global climate. Sci., Vol. 173, No. 3992, 138-141.

Riches, M. R., 1974: A study of the effect of atmospheric aerosols on infrared irradiance at the earth's surface in a non-urban environment. M. S. Thesis, N. C. State Univ., Raleigh, N. C., 54 p.

Robinson, G. D., 1950: Notes on the measurement and estimation of atmospheric radiation. Quart. J. Roy. Meteor. Soc., Vol. 76, No. 327, 37-51.

Robinson, G. D., 1962: Absorption of solar radiation by atmospheric aerosol, as revealed by measurements at the ground. Arch. Meteor. Geoph. Biokl., Ser. B, Vol. 12, No. 1, 19-40.

Rouse, W. R., Noad, D., and McCutcheon, J., 1973: Radiation, temperature and atmosphere emissivities in a polluted urban atmosphere at Hamilton, Ontario. J. Appl. Meteor., Vol. 12, No. 5, 798-807.

Sargent, S. L., and Beckman, W. A., 1973: A numerical model of thermal radiation in a dusty atmosphere. J. Atmos. Sci., Vol. 30, No. 1, 88-94.

Sasamori, T., 1968: The radiative cooling calculation for application to general circulation experiments. J. Appl. Meteor., Vol. 7, No. 5, 721-729.

Sellers, W. D., 1965: Physical Climatology. Univ. of Chicago Press, Chicago, Illinois.

Sheppard, P. A., 1958: The effect of pollution on radiation in the atmosphere. Int. J. Air Poll., Vol. 1, No. 1, 31-43.

Staley, D. O., and Jurica, G. M., 1972: Effective atmospheric emissivity under clear skies. J. Appl. Meteor., Vol. 11, No. 2, 349-356.

Swinbank, W. C., 1963: Long-wave radiation from clear skies. Quart. J. Roy. Meteor. Soc., Vol. 89, No. 381, 339-348.

Twitty, J. T., and Weinman, J. A., 1971: Radiative properties of carbonaceous aerosols. J. Appl. Meteor., Vol. 10, No. 4, 725-731.

Volz, F. E., 1972a: Infrared absorption by atmospheric aerosol substances. J. Geophys. Res., Vol. 77, No. 6, 1017-1031.

Volz, F. E., 1972b: Infrared refractive index of atmospheric aerosol substances. Appl. Optics, Vol. 11, No. 4, 755-759.

Winkler, P., 1973: The growth of atmospheric particles as a function of relative humidity - an improved concept of mixed nuclei. J. Aerosol Sci., Vol. 4, No. 5, 373-387.

Yamamoto, G., 1952: On a radiation chart. The Sci. Rep. of the Tokyo Univ., Ser. 5, Geophy., Vol. 4, No. 1, 9-23.

TECHNICAL REPORT DATA
(Please read Instructions on the reverse before completing)

1. REPORT NO.	2.	3. RECIPIENT'S ACCESSION NO.
EPA-650/4--75-017		

4. TITLE AND SUBTITLE	5. REPORT DATE
Effects of Atmospheric Aerosols on Infrared Irradiance at the Earth's Surface in a Nonurban Environment	May 1975
	6. PERFORMING ORGANIZATION CODE

7. AUTHOR(S)	8. PERFORMING ORGANIZATION REPORT NO.
M.R. Riches, J.T. Peterson, and E.C. Flowers	

9. PERFORMING ORGANIZATION NAME AND ADDRESS	10. PROGRAM ELEMENT NO. 1AA009
Meteorology Laboratory Environmental Protection Agency Research Triangle Park, N.C. 27711	ROAP No. 26AAS
	11. CONTRACT/GRANT NO.

12. SPONSORING AGENCY NAME AND ADDRESS	13. TYPE OF REPORT AND PERIOD COVERED
Same	14. SPONSORING AGENCY CODE

15. SUPPLEMENTARY NOTES

16. ABSTRACT

This report describes a study designed to measure hemispheric infrared downward-directed irradiance at the earth's surface and ambient aerosol concentrations at Research Triangle Park, North Carolina. A Funk-type net radiometer (with a blackened cavity on the underside) was used to measure the incident all-wave energy. From the value obtained, the observed solar radiation was subtracted to determine the infrared component. The expected incident infrared irradiance was calculated from prevailing atmospheric conditions. Six methods were used for these calculations: four empirical equations based on surface conditions, the Yamamoto chart, and a radiative transfer program using vertical profiles of temperature and moisture. The observed-minus-calculated downwelling irradiances were then compared to concurrent measurements of turbidity obtained with a Volz sunphotometer, nephelometer-indicated atmospheric extinction coefficient, and relative humidity. These measurements were analyzed by least-squares regression to determine the extent to which incident hemispheric infrared radiation is affected by varying amounts of atmospheric aerosols and relative humidity.

17. KEY WORDS AND DOCUMENT ANALYSIS

a. DESCRIPTORS	b. IDENTIFIERS/OPEN ENDED TERMS	c. COSATI Field/Group
Infrared irradiance aerosols turbidity solar radiation atmospheric extinction coefficient relative humidity		

18. DISTRIBUTION STATEMENT	19. SECURITY CLASS *(This Report)*	21. NO. OF PAGES
Release unlimited	none	42
	20. SECURITY CLASS *(This page)*	22. PRICE
	none	

EPA Form 2220-1 (9-73)

ENVIRONMENTAL PROTECTION AGENCY
Technical Publications Branch
Office of Administration
Research Triangle Park, N.C. 27711

OFFICIAL BUSINESS

AN EQUAL OPPORTUNITY EMPLOYER

POSTAGE AND FEES PAID
ENVIRONMENTAL PROTECTION AGENCY
EPA - 335

U.S. MAIL

Return this sheet if you do NOT wish to receive this material ☐, or if change of address is needed ☐ (Indicate change, including ZIP code.)

PUBLICATION NO. EPA-650-/4-75-017